PNNL-36530
M3LW-24OR0404023

Light Water Reactor Sustainability Program

Evaluation of Clamshell Current Coupler for Online Frequency Domain and Spread Spectrum Time Domain Reflectometry to Detect Anomalies in Energized Cables

S.W. Glass, J. Tedeschi, M. Elen, M.P. Spencer, J. Son, V. Kumar, L.S. Fifield
Pacific Northwest National Laboratory

September 2024

U.S. Department of Energy
Office of Nuclear Energy

DISCLAIMER

This information was prepared as an account of work sponsored by an agency of the U.S. Government. Neither the U.S. Government nor any agency thereof, nor any of their employees, makes any warranty, expressed or implied, or assumes any legal liability or responsibility for the accuracy, completeness, or usefulness, of any information, apparatus, product, or process disclosed, or represents that its use would not infringe privately owned rights. References herein to any specific commercial product, process, or service by trade name, trademark, manufacturer, or otherwise, does not necessarily constitute or imply its endorsement, recommendation, or favoring by the U.S. Government or any agency thereof. The views and opinions of authors expressed herein do not necessarily state or reflect those of the U.S. Government or any agency thereof.

PNNL-36530
Milestone #: M3LW-24OR0404023

Evaluation of Clamshell Current Coupler for Online Frequency Domain and Spread Spectrum Time Domain Reflectometry to Detect Anomalies in Energized Cables

S.W. Glass, J. Tedeschi, M. Elen, M.P. Spencer, J. Son, V. Kumar, L.S. Fifield

Pacific Northwest National Laboratory

September 2024

Prepared by
Pacific Northwest National Laboratory
Richland, WA 99354
operated by
Battelle
for the
U.S. Department of Energy
Under Contract DE-AC05-76RL01830

SUMMARY

This document describes adaptation and evaluation of a clamshell inductive current coupler for online reflectometry testing (both frequency domain reflectometry and spread spectrum time domain reflectometry) to evaluate cable insulation degradation and anomalies. Safety-critical nuclear power plant cables were initially qualified for 40 years. However, as plants extend their operating licenses to 60 and 80 years, justification for continued safe operation includes test and monitoring programs. These will become more important as the industry moves to condition based qualification programs. Cable test programs traditionally involve manual interventions to disconnect cables, perform one or several tests, then reconnect the systems, usually during refueling outages occurring only every 18 to 24 months. This poses an operational burden that can be minimized by online testing or periodic connection to a coupler that may remain on the cable of interest or be clamped onto the cable without de-termination. This work investigates the adaptation of a clamshell inductive current coupler for either frequency domain reflectometry or spread-spectrum time domain reflectometry. The reflectometry test instrument injects a broad-band chirp or pseudo-noise signal onto a cable conductor and monitors for a reflected signal indicative of an impedance change caused by a damage condition. The instrument maximum input signal levels are typically 10 to 30 volts or less and the instruments will be damaged if subjected to 60 Hz power line voltages of 110, 220, or 480 VAC. One commercial spread-spectrum time domain reflectometry system has circuitry suitable for voltages up to 1 kV, but typical reflectometry tests are performed on de-energized cables. The clamshell inductive coupler provides >60 dB of 60 Hz attenuation with less than 10 dB loss in the 1-500 MHz test bandwidth of interest. An energized cable was successfully tested up to 6.7 kVp-p and frequency response plots imply that the tests could be extended to 10 kV or higher energized levels.

ACKNOWLEDGEMENTS

This work was sponsored by the U.S. Department of Energy, Office of Nuclear Energy, for the Light Water Reactor Sustainability (LWRS) Program Materials Research Pathway. The authors extend their appreciation to Pathway Lead Dr. Xiang (Frank) Chen for LWRS programmatic support. This work was performed at the Pacific Northwest National Laboratory (PNNL). PNNL is operated by Battelle for the U.S. Department of Energy under contract DE-AC05-76RL01830. The authors would like to thank Matthew Prowant, and Stephen Jones for their assistance in this work.

CONTENTS

FIGURES

TABLES

ACRONYMS

AC	alternating current
ARENA	Accelerated and Real-Time Environmental Nodal Assessment
AWG	arbitrary waveform generator
BPSK	binary phase shift keying
BW	bandwidth
DAQ	data acquisition (as referring to DAQ leader cable)
DC	direct current
Fc	carrier frequency
EMI	electromagnetic interference
EPR	ethylene propylene rubber
FDR	frequency domain reflectometry
FMCW	frequency modulated continuous wave
FFT	fast Fourier transform
IL	insertion loss
NPP	nuclear power plant
PN code	pseudo-random noise code
PNNL	Pacific Northwest National Laboratory
RF	radio frequency
SRSS	square root sum of squares
SSTDR	spread spectrum time domain reflectometry
V	volt
Vp-p	peak-to-peak voltage
VAC	volts alternating current
VNA	vector network analyzer

1. INTRODUCTION

There is a need for active interrogation methods to probe safety-critical energized cables for conductor and insulation damage or degradation that may threaten cable reliability. Cable degradation can occur due to a number of factors including heat, moisture, chemical exposure, radiation, flexure, abrasion, pinching, plus connector and splice crimp workmanship issues. All these factors can lead to cable insulation materials crumbling, separating, eroding, degrading dielectric insulation properties, or breaking and exposing conductors that may lead to low-resistance, short or open circuits and corresponding circuit failures with associated safety risks and/or operational outages. Cable monitoring tests are most helpful if they can detect early damage indications well before system failures and can localize the areas of interest to guide supplemental inspections and damage management actions.

Radio frequency (RF) reflectometry methods utilize high-frequency signals over a broad frequency range (typically from kHz to hundreds of MHz) to reveal information on the cable structure as a function of location along the cable. Although no single cable test can assure detection of all damage mechanisms, these high-frequency approaches can be applied without affecting low-frequency or direct current (DC) power applications and can not only detect but also locate indications of concern.

Reflectometry tests are normally performed on un-energized cables. In some cases, tests are applied without decoupling the cable. Frequently, however, the cables are decoupled from one or both termination ends for the test. Not only is this an inconvenience for plant operators but it opens the system to re-connection workmanship errors. Moreover, operators are understandably concerned about physically connecting test equipment to cable conductors on safety critical systems. The inductive clamshell coupler can mitigate or eliminate these concerns.

Online cable test technology and experience for nuclear power plants is limited (Glass et al. 2020). Partial discharge testing may be used on critical systems but is most commonly applied to service critical medium and high voltage transmission and distribution lines (Ahmed and Srinivas 1998, Han et al. 2023). Commercial reflectometry systems have been widely applied to low voltage aircraft and electric rail systems but have not been broadly used in nuclear plants (Glass et al. 2020). Fiber optic systems are used for both onshore and offshore high voltage distribution lines but are rarely found on the low or medium voltage systems typical of nuclear plants. This work is primarily focused on low and medium voltage reflectometry tests that may be developed into nuclear power plant online monitoring systems. However, the technology may have significantly broader potential for other safety critical cable monitoring.

2. FREQUENCY DOMAIN REFLECTOMETRY

Frequency domain reflectometry (FDR) is being used in nuclear plants, particularly to locate areas of concern on de-energized cables. The FDR instrument, typically based on a vector network analyzer, is connected to two cable conductors, one considered the primary conductor under test and the other considered the system ground, as shown in Figure 1. This is referred to as a "T" connection, which will typically produce a reflection from the connection of the FDR lead wire to the cable under test. The FDR instrument directs a swept frequency chirp onto a conductor then listens for any reflection from an impedance change along the cable length or to a parallel conductor within the cable bundle (Glass et al. 2017). Significant noise immunity and sensitivity to subtle impedance changes can be achieved by listening and detecting the reflections in the frequency domain, filtering, and converting to the time domain with an inverse Fourier transform. The signal may then be transformed to the distance domain using the velocity of propagation characteristic of the cable [1]. The bandwidth for FDR is software adjustable, but experience shows the best responses occur from 50 MHz to 500 MHz. Higher bandwidth FDR signals produce sharper peaks capable of spatially resolving more closely spaced impedance changes. The higher frequencies, however, do not propagate as far along the cable length due to signal attenuation. Testing is performed at multiple bandwidths providing analysts with both high- and low-frequency bandwidths to consider in dispositioning test results. FDR instruments are generally restricted to relatively low voltages and cannot tolerate testing on energized cable systems. One exception to this is the commercial Wirescan company who recently claimed to be able to couple to energized lines up to 33 kV [2]. This coupling also connects to the primary conductor via a "T" connection with both capacitive and inductive pickups. Details of this design are proprietary to Wirescan.

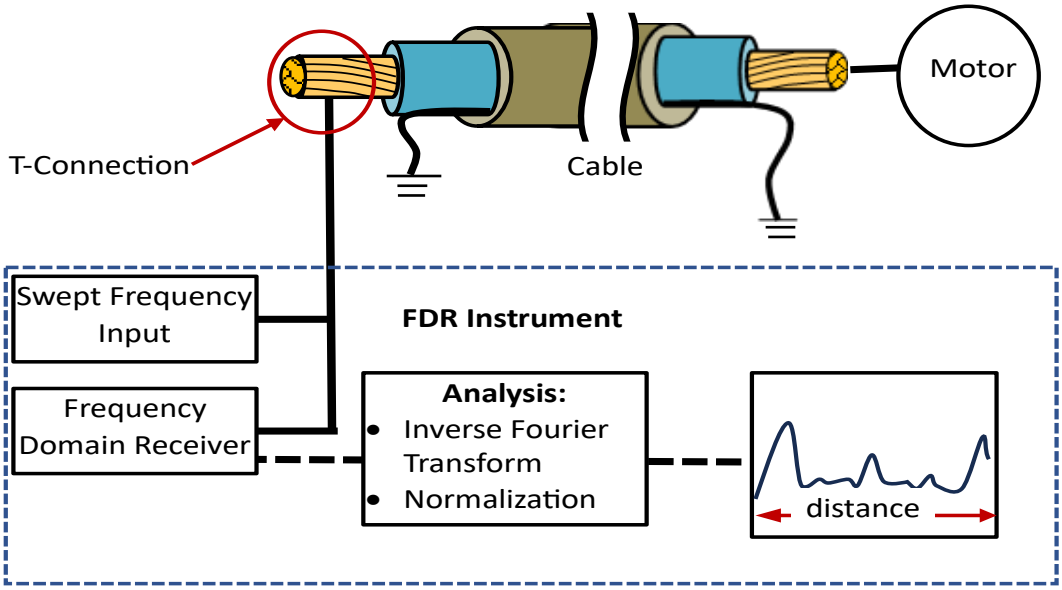

Figure 1. The FDR cable test introduces a swept frequency chirp onto a conductor and then listens for any reflection from impedance changes along the cable length.

3. SPREAD SPECTRUM TIME DOMAIN REFLECTOMETRY

Spread spectrum time domain reflectometry (SSTDR) produces a similar plot to FDR, but all processing is in the time domain (Furse 2006). A pseudo-random noise (PN) code modulated with a square wave carrier through a high-pass filter is input onto the cable conductor, also via a "T" connection, and the instrument listens for any reflected response from cable anomalies (see Figure 2). The SSTDR processes the signal by performing a cross-correlation, comparing the input PN code to any reflected signal detected. The cross-correlation algorithm produces a robust noise-tolerant signal response like FDR, essentially when using a matched filter approach. The effective bandwidth vs. modulation bandwidth is different for FDR than it is for SSTDR. Where FDR utilizes a frequency modulated continuous wave (FMCW) chirp, sweeping over a bandwidth with very sharp edges at the start/stop of the chirp, SSTDR modulates a carrier with a specific modulation frequency equating half of the 3 dB bandwidth (e.g. 20 MHz modulation equates to ~40 MHz of bandwidth). However, there are subtleties in the SSTDR bandwidth definition as the edges are not sharp start/stop points as in the FDR case; they gradually roll off with SSTDR and thus create a wider effective bandwidth that can be used for fine time domain resolution. With these differences, generalizations about lower vs. higher bandwidth still apply.

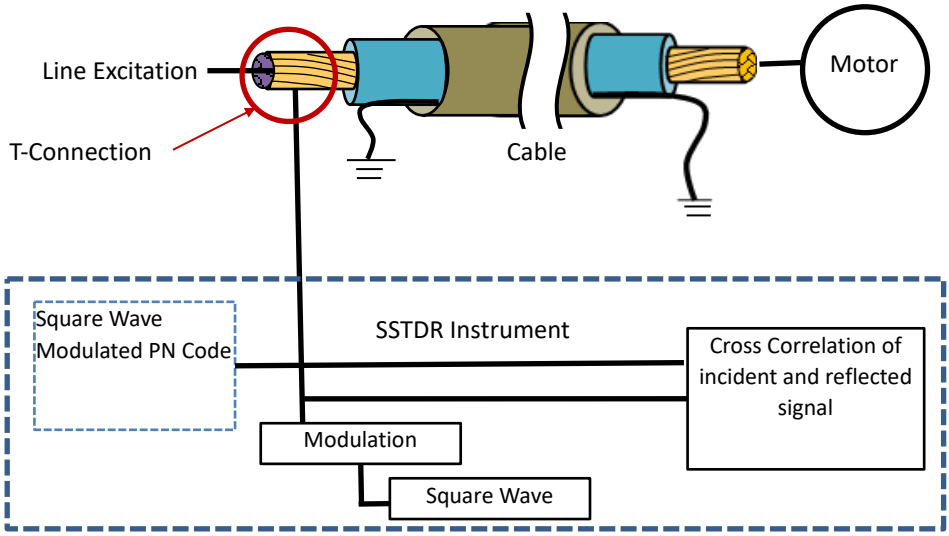

Figure 2. SSTDR cable test applies a PN code to the conductor for cross-correlation analysis.

Currently, SSTDR is offered commercially through LiveWire Innovation. One distinct advantage of the LiveWire SSTDR is that the circuitry can be used for measurements on energized cable up to 1 kV. The LiveWire instrument, however, is hardware limited to frequency bandwidths of 48 MHz. To permit higher bandwidths to be examined, a custom, laboratory-grade SSTDR was implemented using an arbitrary waveform generator to create spread spectrum waveforms and a digitizing oscilloscope to capture the reference and return signals (Glass et al. 2023). The digitized signals were then processed in Python-based implementations of a cross correlation function with custom frequency domain windowing. This laboratory instrument SSTDR extended the bandwidth up to 500 MHz, although actual cable tests were quite noisy and therefore uninteresting for bandwidths above 200 MHz on 100 ft cables.

4. INDUCTIVE CURRENT PROBE

The laboratory instrument SSTDR, vector network analyzer FDR, and most other RF instruments have an input limit of 10 to 30 Volts at 60 Hz. Without a protection/isolation circuit, high-voltage DC or 60 Hz alternating current (AC) voltage (typically from 120 V to 15 kV) will damage costly RF test equipment. An ideal way to perform these measurements is with a high-pass filter that can suppress DC and 60 Hz low-frequency power voltages and allow higher RF signals to pass through. It is, however, not practical to support both high-voltage suppression and passing of high RF signals (>100 MHz) due to frequency/voltage limitations of lumped element circuit components. Therefore, instead of a classical filter, a current probe that supports reciprocal measurements is used in this work. The commercial current probe can both transmit and receive. It can also be used to inject and sense RF signals on a live voltage line while providing low-frequency isolation to RF test equipment.

RF current probes are based on alternating current behavior described by Ampere-Maxwell equations. In the application of a current probe (see Figure 3**)**, an alternating current along the primary conductor, I_P, will induce a magnetic flux, B, within the core of the ferromagnetic material surrounding the primary conductor. A readout conductor is then wrapped around the ferrite core to measure a secondary current, I_s, that is proportional to the number of turns wrapped around the ferromagnetic core, N, in relation to the primary current. The architecture shown in Figure 3 is used for commercial applications of measuring current on AC lines for a single conductor as shown in Figure 4 (Fluke 2022). The design of the core and number of windings influence the characteristic impendence and set the current at which the ferrite core itself will saturate. Specific design considerations also include elements such as parasitic capacitance between secondary windings for high-frequency current probes. RF current probes are transformers that measure or produce a voltage in a 50-ohm load proportional to the current flowing through the probe inner diameter based on the characteristic impedance of the probe. This is referred to as the transfer impedance of the probe and leads to the insertion loss through the probe vs. frequency (Yao et al. 2014) expressed as:

$$IL = 20\log_{10}(R) - Z_T, \qquad \text{Eq. 1}$$

where IL = insertion loss (dB), R = impedance of the RF circuit = 50 ohms, and Z_T = transfer impedance (dB ohms). The insertion loss values through RF probes are in the -40 to -80 dB range for 60 Hz signals, while in the MHz frequency range are typically less than -10 dB. This creates a non-contact, frequency selective probe through which RF signals can interact with live voltage lines.

A standard application for commercial RF current probes is the sensing and investigation of the presence of electromagnetic interference on conductors typically manifesting as stray signals that have coupled onto the lines. Another is the induction of electromagnetic interference (EMI) onto a line to determine the sensitivity of a circuit to external EMI. The use case of the RF current probe in this work is for both transmission and reception of RF signals to perform reflectometry measurements while maintaining both physical and frequency isolation far from the high DC or 60 Hz AC voltage. An A.H. Systems injection current probe ICP-622 (A.H. Systems 2023) was selected (see Figure 5). This product provides an operational RF bandwidth from 1–500 MHz and high isolation from DC and 60 Hz as seen in the insertion loss of the probe in Figure 5. Initial tests with the clamshell coupler revealed a response sensitivity to the conductor being centered and fixed within the coil. A three-dimensional printed plastic centering assembly and absorber shielding was added to the commercial unit to minimize this issue.

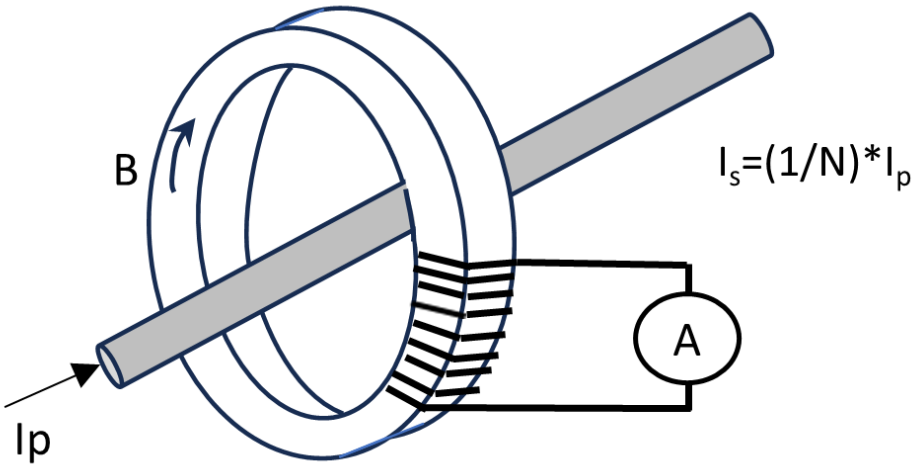

Figure 3. Architecture of a typical current probe.

Figure 4. Example of a commercial clamp-on current probe.

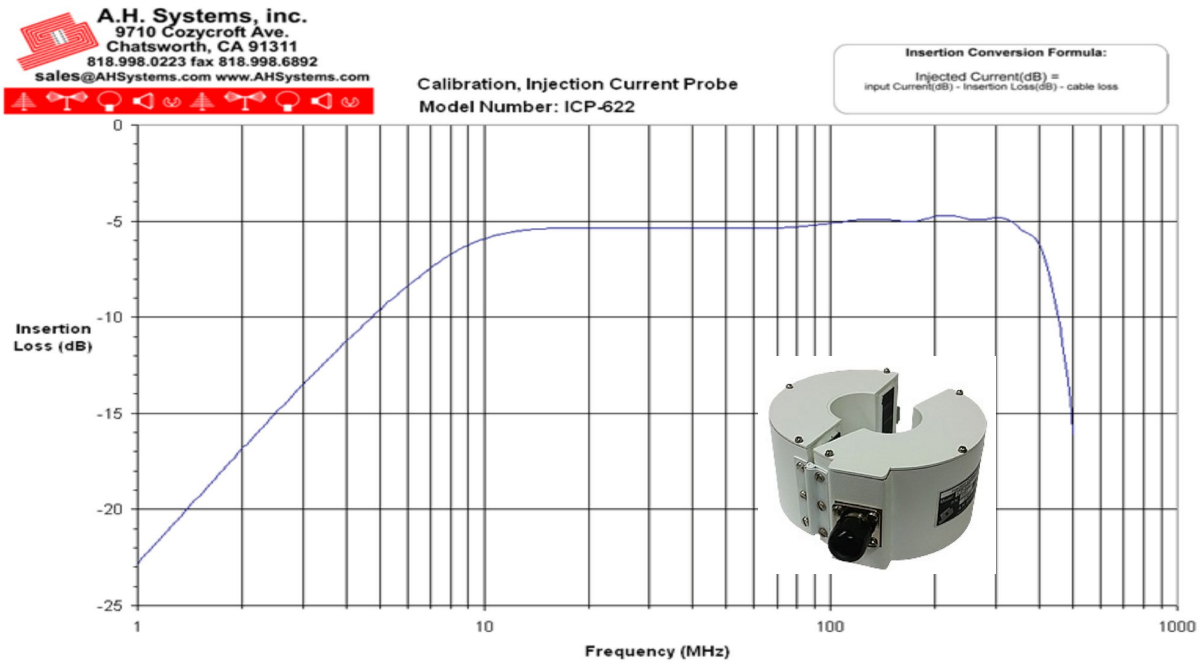

Figure 5. This product provides good response from 1 to 500 MHz with low frequency isolation including operational line frequencies.

5. REFLECTOMETRY TEST using CLAMSHELL COUPLER

Tests of the clamshell coupler consisted of:

- Characterizing the frequency response, particularly focusing on the ability of the coupler to protect measurement instruments from 60 Hz high voltages.
- Contrasting the reflectometry results for a direct cable coupling to the cable conductor, for an unenergized inductive coupling, and for an energized inductive coupling.
    - Medium Voltage Cables
    - Low Voltage Cables

5.1 Characterization of Frequency Response

The isolation of the current probe as a function of frequency was investigated by the test configuration shown in Figure 6. A waveform generator was used to create sine waves from 60 Hz to 80 MHz and the measured voltage peak to peak was compared for each frequency sample between a reference through-path and the output of the current coupler. The ratio of the measure outputs, 20 $\log_{10}$(coupled/through), is shown in Figure 7. As expected, the response drops significantly at 60 Hz and there is minimal loss at frequencies greater than 10 MHz, thus demonstrating the ability of the current coupler to provide frequency selectivity and protect sensitive RF equipment. The voltage isolation ability of the current probe was confirmed on a medium voltage cable rated to 5 kV using a Tan Delta test instrument to inject a 5 kV, 0.1 Hz signal. The cable end responses were clearly visible with both FDR and SSTDR tests and were substantially the same for both the energized and unenergized case.

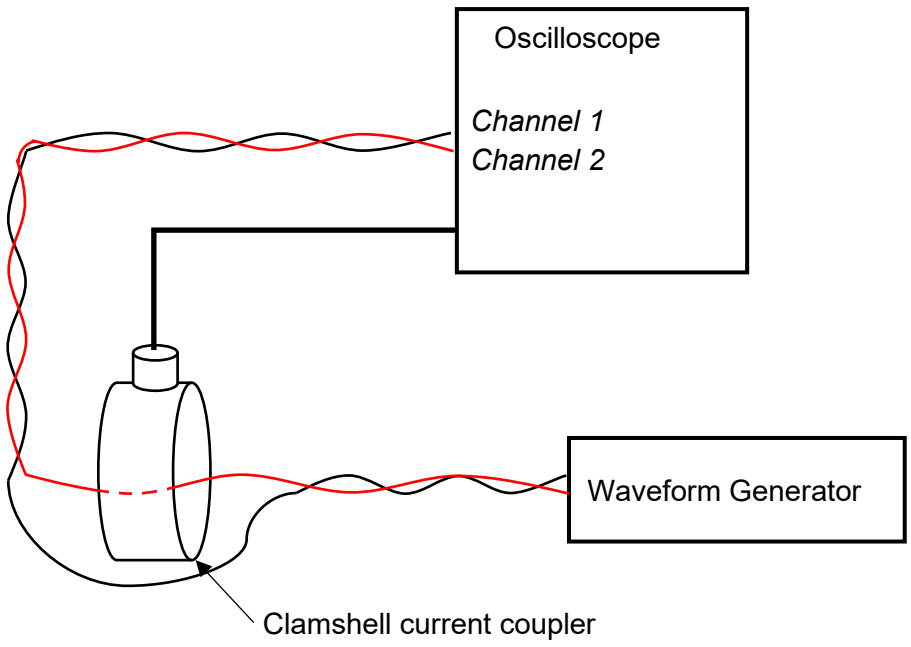

Figure 6. Test arrangement for measuring clamshell current coupler line voltage 60 Hz attenuation.

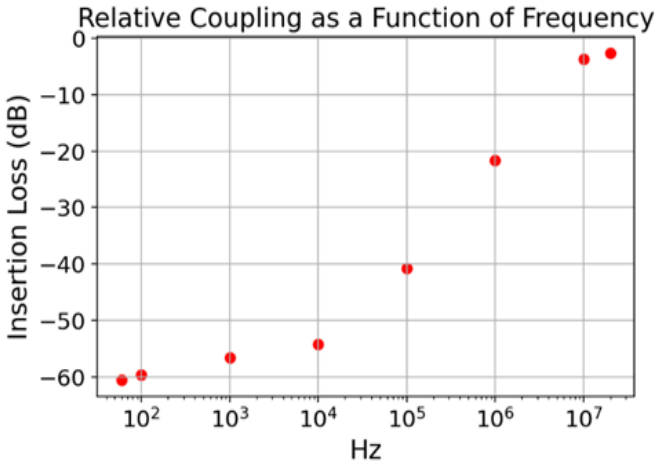

Figure 7. Clamshell current coupler isolation as a function of frequency.

5.2 Medium Voltage Cable Tests

After confirming that the current probe should provide sufficient isolation to protect the reflectometry equipment from live-line voltages, a test configuration was created to prove the concept of an energized FDR test on a medium voltage cable. A 16-ft long OKONITE OKOGUARD medium voltage cable, with jacket description as "2015 OKONITE 4 1/0 AWG COMPACT CU OKOGUARD EP PVC SHLD 5KV 133%-8KV 100% INSUL LEVEL 115 MILS <UL>-MV105 SUN RES FOR CT USE FT -4 -40C OR CSA LR 39608 FT-4 LTDD" was used for this test.

The test configuration is shown in Figure 8, where a 120 VAC (377 Vpp) 60 Hz voltage is stepped up using a Hammond Manufacturing voltage transformer to 2.4 kVAC (6.7 kVpp). The transformer and medium voltage cable were guarded within a plastic enclosure where the outer jacket of the medium voltage cable was removed for the current probe clamp directly around the insulated conductor.

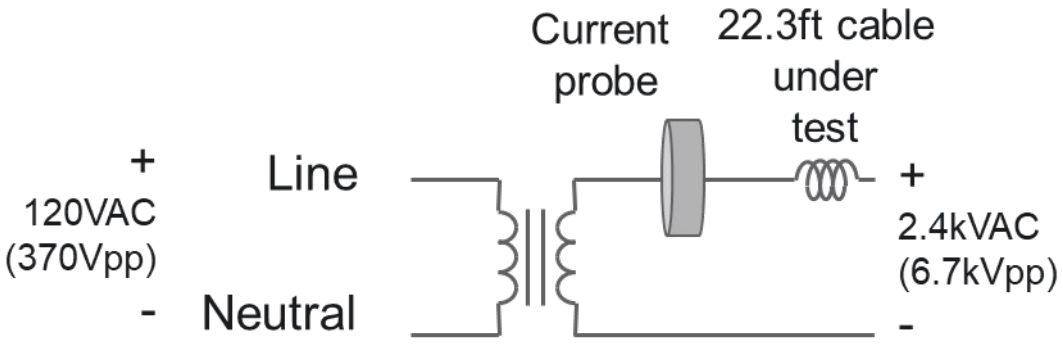

Figure 8. Test configuration for medium voltage cable.

A Fluke high voltage probe capable of measuring AC voltages up to 40 kV was used to confirm the output voltage of the voltage transformer at 2.4 kVAC. The probe, transformer, and cable under test are shown in Figure 9.

Figure 9 Fluke high voltage probe 80K-40 (left), probe measuring transformer output (right).

The clamshell coupler was installed inside the plastic enclosure and connected to the VNA system. Figure 10 below shows the test configuration with the current probe clamped around the medium voltage cable under test and with the connection to the VNA to perform FDR.

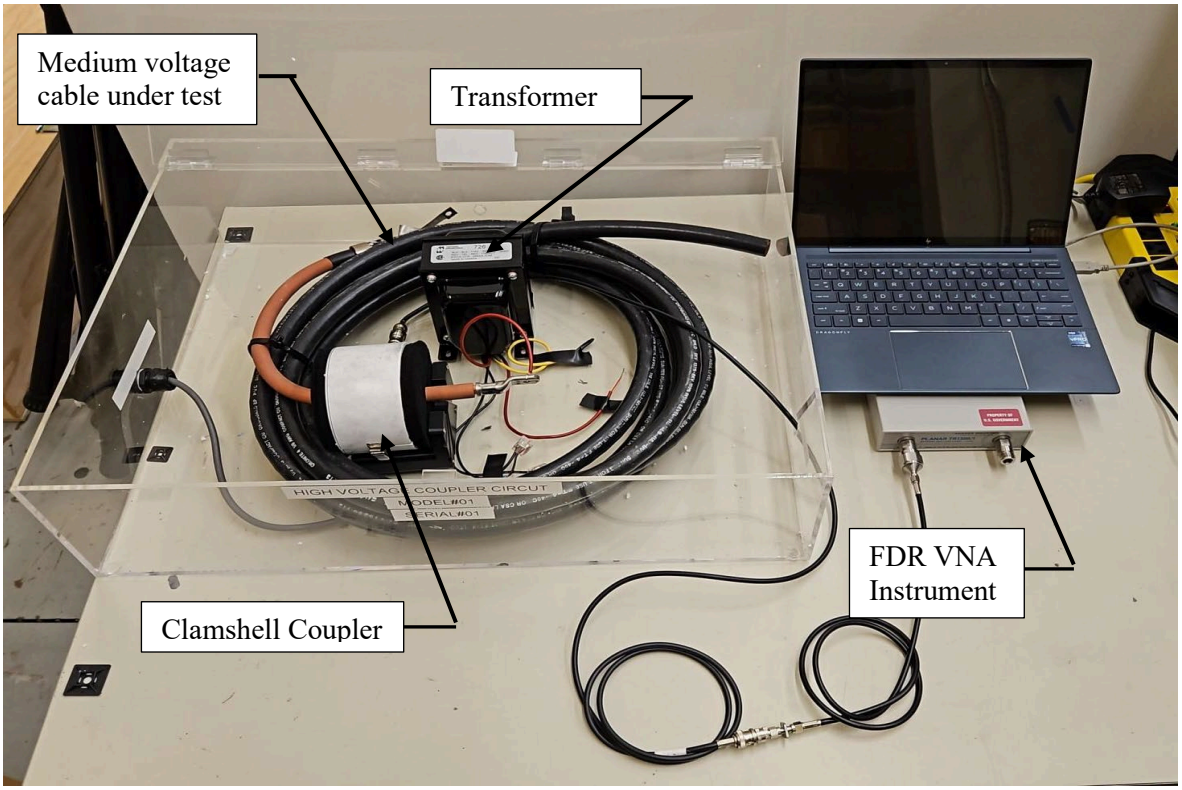

Figure 10. Test configuration for transformer generated 2.4 VAC (6.7 Vp-p) medium voltage energized cable FDR test.

The VNA measured the frequency response from 1-500MHz for the three different hardware states.

1) Transformer disconnected from the test circuit,
2) Transformer connected but de-energized, and
3) Transformer connected and energized.

The measured frequency response was cropped to an optimal bandwidth that coupled efficiently onto the cable under test and highlighted the end of the cable. Figure 11 shows the initial FDR response for the cable under test in the three conditions previously listed. This result demonstrated the ability to perform FDR on an energize medium voltage cable using the inductive clamshell coupler.

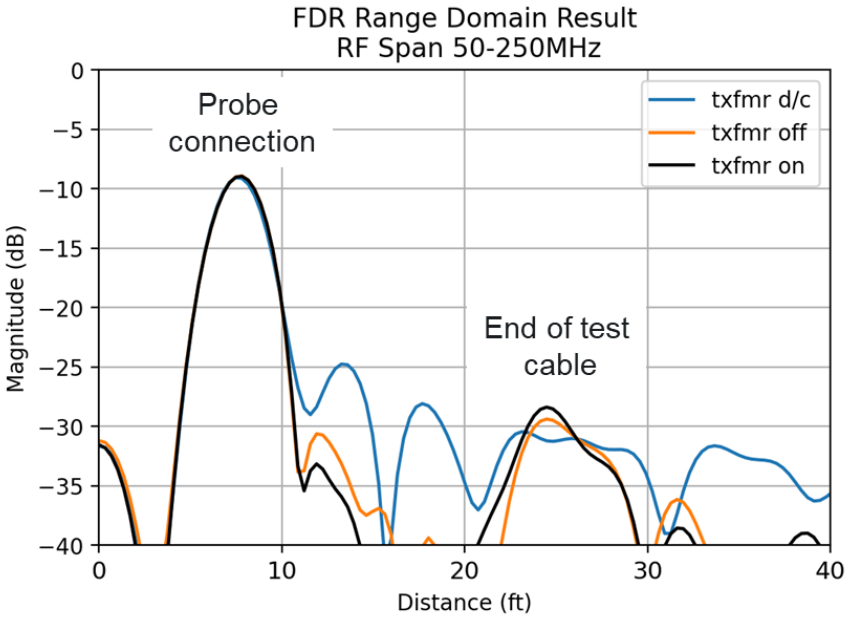

Figure 11. FDR test of 25 ft. long medium voltage cable energized at 2.4 kVAC (6.7 kVp-p). Transformer D/C indicates the test was performed with the unenergized cable direct coupled to the test instrument. Transformer off was the unenergized cable test through the clamshell coupler and transformer on was for the energized cable test through the clamshell coupler.

5.3 Low-Voltage Cable Tests

5.3.1 Experimental Setup

The clamshell coupler was tested on various damaged and undamaged cables in both the energized and unenergized conditions. The test setup is shown in Figure 12 and includes an approximately 20-ft leader cable from the instrument to the "T" coupling or the inductive coupling. Reflectometry sends chirp excitation and receives reflection signals equally in both directions. Closing an energizing switch exposes the reflectometry signal to upstream power line branches, "Ts", splices, and other supply cable anomalies that can reflect and appear on the reflectometry response plot. These may not be readily distinguishable from anomalies in the cable under test. Tests were performed on the ARENA cable / motor test bed (Glass et al. 2021) which supported 480 volts alternating current (VAC) three-phase energized and un-energized tests of low-voltage ethylene propylene rubber (EPR) cable as shown in Table 1. The cable length for both the non-shielded and shielded cables was 62 ft. This length was arbitrarily selected for the cable to be connected to the main circuit, to make a full loop in the ARENA cable test bed cable tray, and to be connected to the motor on the other end.

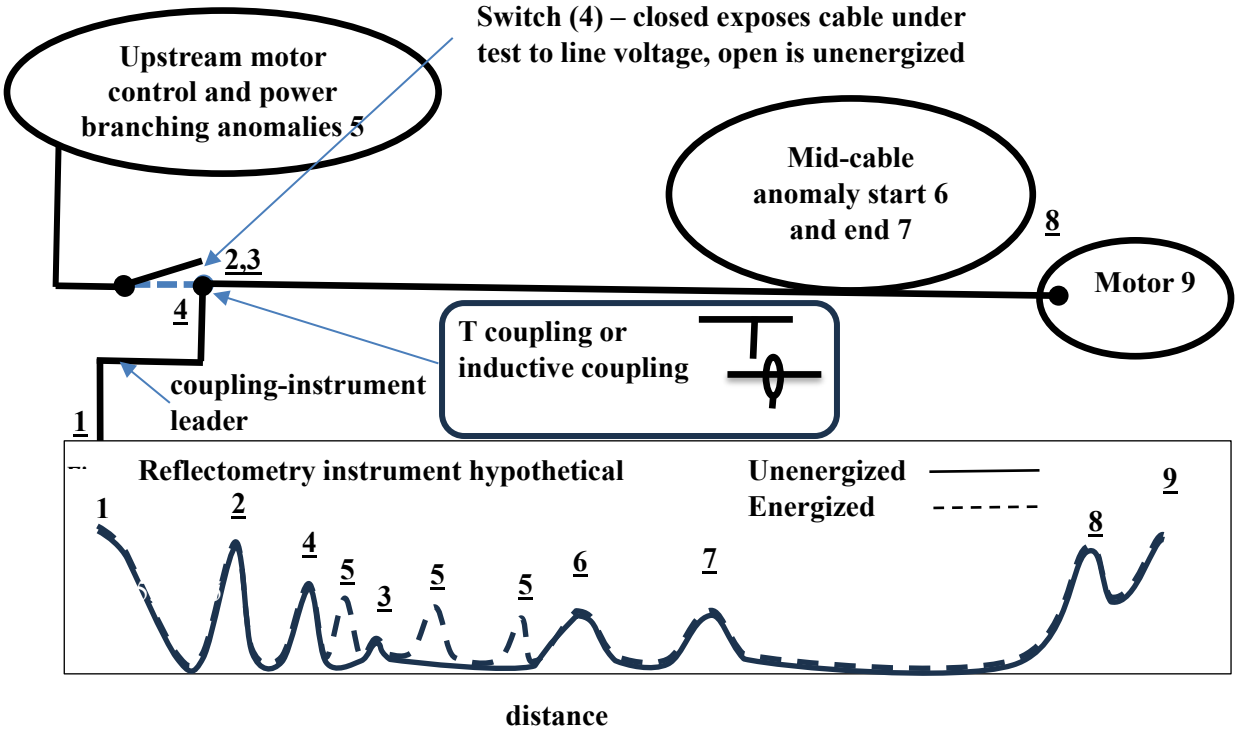

Figure 12. Reflectometry test setup for energized and unenergized cable. Energized tests can show additional response peaks compared to unenergized tests. Numbered features in the circuit diagram correspond to peaks in the hypothetical response plot.

Table 1. Low-voltage cables tested with the clamshell current coupler.

Manufacturer	Insulation	Jacket	Shield
General Cable	EPR	CPE	Yes
Manufacturer designation: 6-903-SH 14AWG-3/C FR-EP 600V FR-EPR/CPE Foil Shielded 600V E-2			
General Cable	EPR	CPE	No
Manufacturer designation: 6-903-G 14AWG-3/C FR-EP 600V FR-EPR/CPE Non-Shielded 600V E-2			

The following equipment configurations of FDR and SSTDR were carried out for both the shielded and non-shielded cables.

- Direct connect – Instruments were directly connected to the cable using the 20ft leader cable – for un-energized measurements.
- Clamshell Coupler connect – Instruments were connected using the 20ft leader cable to the clamshell coupler, and the insulation under test was placed inside the clamshell coupler – as shown in Figure 13 for both un-energized and energized measurements.

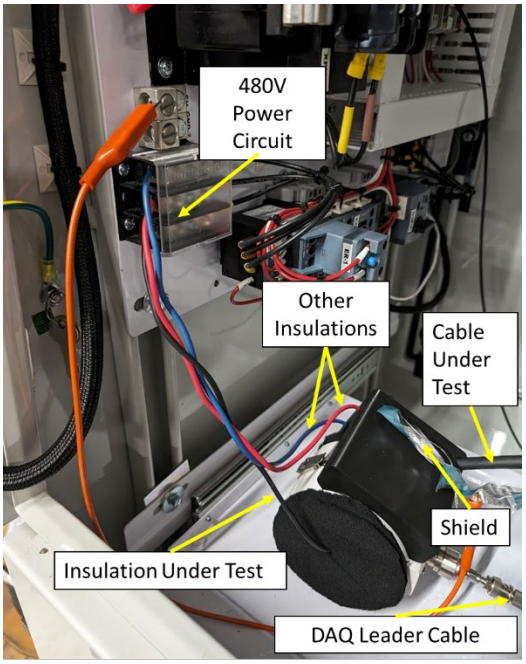

Figure 13. Clamshell coupler setup on shielded cable for energized testing connected to a 480-V source.

In addition to the different equipment configurations described above, different test conditions were also studied. Each end of the Cable was marked as End A and End B. For each measurement one of the ends was connected to the equipment configurations and the other end was as per the following setup.

- Connect End A - Open End B
- Connect End A - Short End B
- Connect End B - Open End A
- Connect End B - Short End A
- Connect End A - End B Connected to Motor

Further, to identify the fault, the following connection variation were made.

- Undamaged Cable
- Damaged Cable at 20 ft from End A
- 400 Ohms resistor Fault at 20 ft from End A
- 600 Ohms resistor Fault at 20 ft from End B

Note that for measurements taken with End B connected, the fault should appear at 42 ft in the plots. Also, for the “Short End” test conditions, energized measurements were not obtained. In Summary, 2 different cable types (Shielded and Non-Shielded), 2 instruments (FDR and SSTDR), 3 different equipment configurations (Direct connect Un-Energized, Clamshell Un-Energized, Clamshell Energized), 5 different test conditions, and 4 different fault conditions were tested, resulting in a total of 208 measurements for the 62-ft cable.

5.3.2 Data Processing

The raw data for both reflectometry methods were collected including both the real and imaginary parts, from which the magnitude raw data (square root sum of squares (SRSS) of real and imaginary parts) is obtained. The magnitude raw data are in arbitrary units (A.U.). The FDR magnitude raw data for bandwidths of 50, 100, 200, and 400 MHz are shown on the left sides of Figure 14 and Figure 15. Note that the anomaly peak is present but would be difficult to identify from the raw data. Also, the energized signal is similar but not identical to the un-energized plot. Various signal-processing approaches are possible, but a relatively clear peak is readily identified using the signal-processing strategy outlined in Table 2. The test leader is first subtracted to focus on the cable under test. The baseline is subtracted. If no baseline is available, a simulated baseline or the first measurement available where the cable is assumed to be good may be used. When test experts analyze the data, they normally consider multiple bandwidths. One way to consider multiple bandwidths in a single plot is to multiply several bandwidths together as indicated in step 4. This seems to accentuate significant peaks and suppress noise. Finally, the complex-number plots are reduced to an SRSS magnitude.

Table 2. Outline of signal processing procedure.

(1) Eliminate leader: The first 20 ft leader cable data (data between coupler and instrument) is removed to focus only on the cable under test for all bandwidths.
(2) Subtract baseline: The similarly processed baseline is subtracted from the measurement of interest for all bandwidths.
(3) SRSS magnitude: The complex number is then processed as a square root sum of squares (SRSS) for a single magnitude response.
(4) Combine bandwidths: A mix of lower and higher frequency bandwidths are then combined (multiplied) to further reduce noise and accentuate reflections of interest.

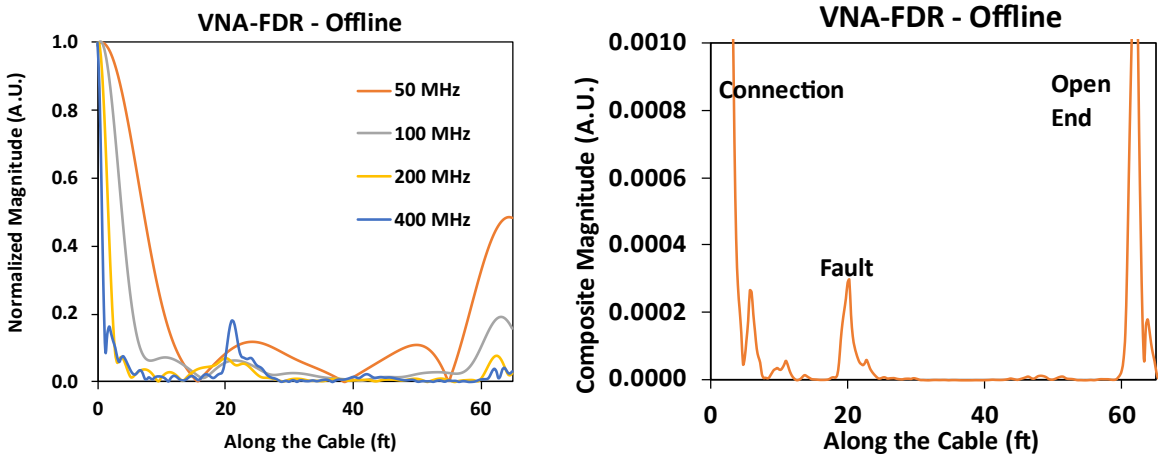

Figure 14. (Left) 50,100, 200, and 400 MHz bandwidth FDR raw responses directly coupled to the unenergized cable (no coupler). (Right) Baseline subtracted combined signal with 50,100, 200, and 400 MHz bandwidths multiplied showing a significantly more visible fault peak. In this case, the fault was a 600-ohm resistor shunt between the cable under test and another phase conductor.

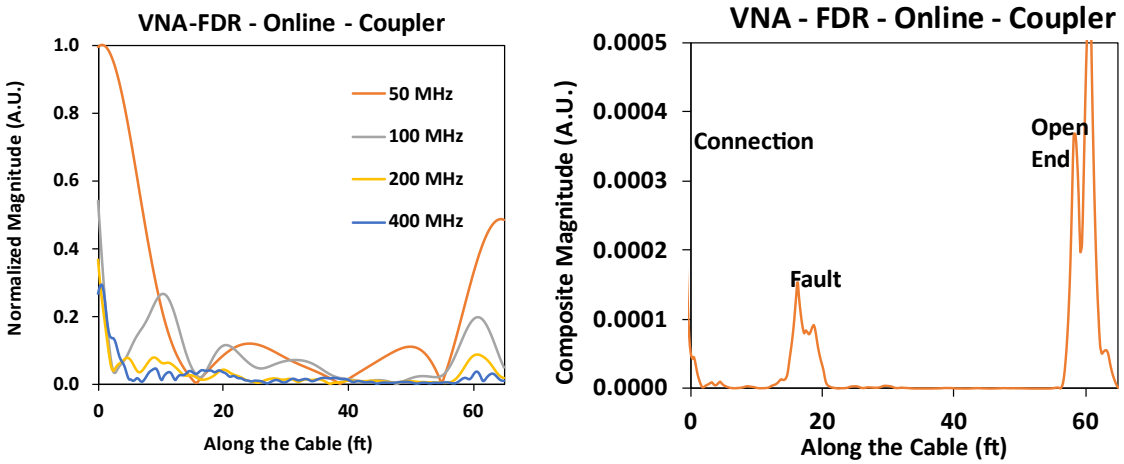

Figure 15. (Left) Multiple bandwidth FDR responses using the clamshell coupler on a 480-VAC energized cable. (Right) Baseline subtracted, combined signal with product of the bandwidths showing a significantly clearer fault peak. The fault was 600-ohm shunt from cable under test to another phase conductor.

5.4 Reflectometry Results

Due to the large volume of data collected for FDR and SSTDR reflectometry, the results are summarized by comparing different test configurations, measurement systems, and their reflectometry responses.

5.4.1 Comparison of Undamaged, Damaged, 400-ohm and 600-ohm resistor faults on a 62-ft Shielded Cable

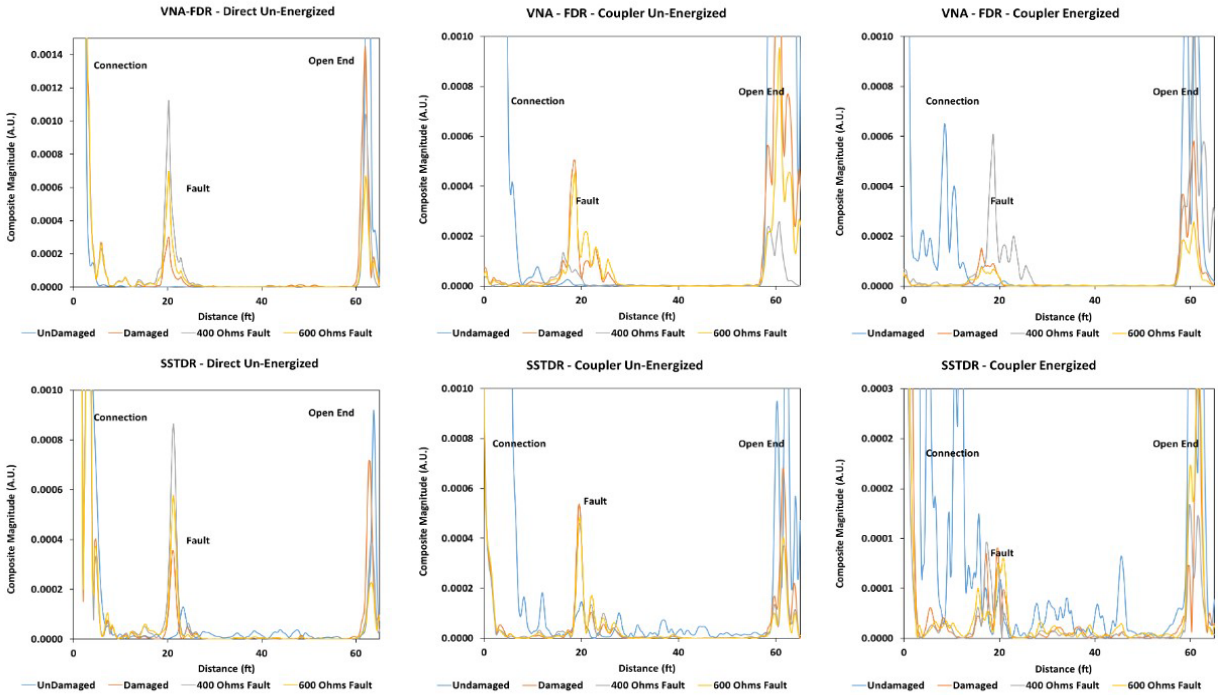

Figure 16. Different fault types compared to the Undamaged 62-ft Shielded Cable for FDR and SSTDR subtracted reflectometry responses in direct connect, coupler-un-energized, and coupler energized configurations.

Figure 16 depicts the composite waveform of the damaged fault reflectometry responses, subtracted from the baseline, and processed as per the data processing procedure listed above. The undamaged response in Figure 16 is the "raw" response, which serves as a baseline, used to subtract the damaged raw responses. Hence the undamaged response has several noise peaks that are eliminated by the process of subtraction and multiplication in the responses of the damaged cable. It can be observed from Figure 16, that the fault–damaged, 400-ohm and 600-ohm resistor can be detected when it is directly connected to the measuring instruments, connected using the clamshell current coupler un-energized, and when the circuit cable is being energized. While comparing the clamshell coupler responses of un-energized vs. energized, several other noise peaks are observed due to the reflections in the energized cable, as depicted in Figure 12.

5.4.2 Comparison of End A and End B Responses of Clamshell Coupler for 600-Ohm Fault Case in a 62-ft Shielded Cable

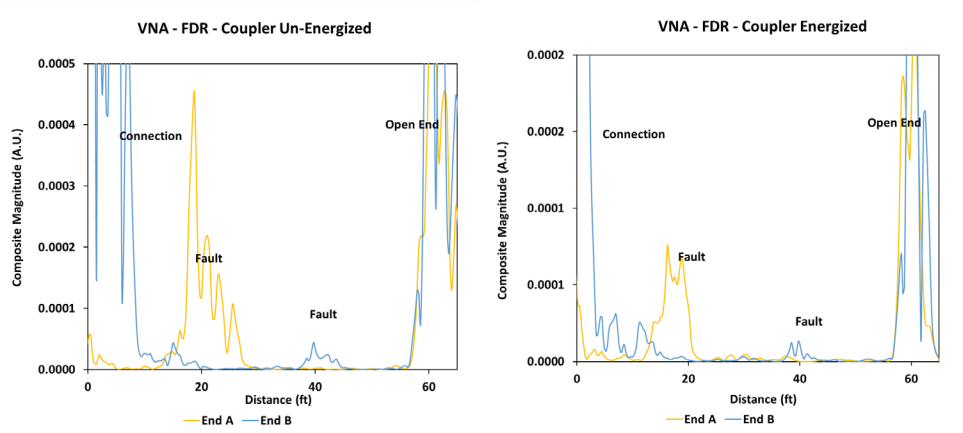

Figure 17. Un-energized and energized composite waveforms of VNA FDR – obtained with clamshell coupler measured from End A and End B, fault located at 20ft from End A, appearing 40 ft from End B.

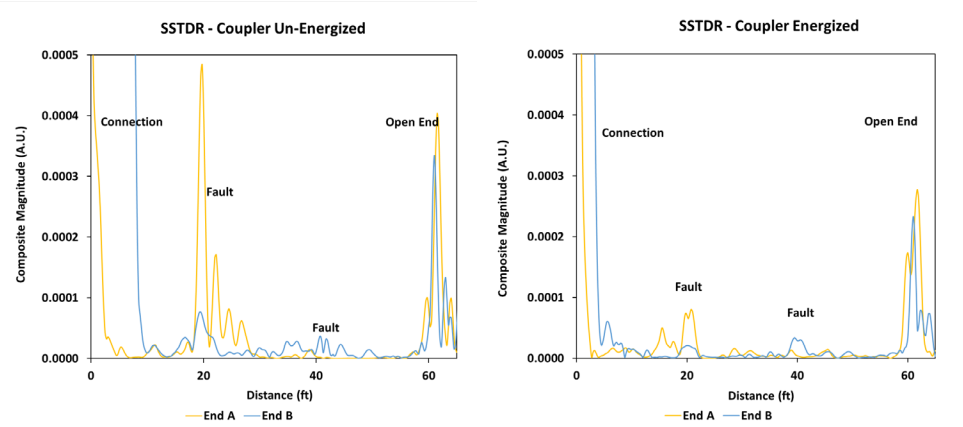

Figure 18. Un-energized and energized composite waveforms of PNNL SSTDR – obtained with clamshell coupler measured from End A and End B of the cable, fault located at 20 ft from End A, which appears at 40 ft from End B.

Figures 17 and 18 depict that the damage faults are visible when measured from both ends of the cable, showing promising results irrespective of the location of the fault in the cable, for both energized and un-energized case.

6. OBSERVATIONS and DISCUSSION

Data interpretation and identification of reflectometry peaks within raw data are difficult. Indications of anomaly reflections seem to be present within multiple bandwidths, but no clear peak rises above the background noise level using the raw data for many of the fault conditions including those shown. Processing of the data, however, results in a clearer peak associated with an anomaly of interest. The clamshell coupler signal quality is quite similar to the direct-coupled responses.

The reflectometry chirps propagate the excitation signal equally in both directions along the cable. If the coupler is installed near the cable end, the chirp includes both the signal propagated directly along the cable section under test and also the reflected signal from the cable end close to the coupler. If the coupler is well removed from a cable end, the signal will propagate equally in both directions along the cable. With a single sensor, the reflected signal peaks can be from either the cable under test or from a reflector within or beyond the motor controller or system actuator switch. If the reflection is from an impedance change within the controller or upstream from this switch, its potential for confusion with anomalies of concern may be mitigated by baseline subtraction so long as the same signal is present within the baseline.

The clamshell coupler offers significant operational advantages, including the ability to both inject and receive signals without direct contact with cable conductors. The tests described herein demonstrated connected to a line energized at 6.7 kVp-p but the coupler may effectively isolate test instruments from significantly higher voltage systems as indicated by the frequency response test. The >60 dB signal drop @ 60 Hz would reduce a 10 kV line voltage to less than 10 V – i.e. within the rated voltage of both SSTDR and FDR instruments.

The clamshell coupler must be installed on an unshielded portion of the cable. If installed over a shield, the injected chirp will only be propagated along the shield. Applying the coupler for reflectometry monitoring requires adjusting the shield cut-back near a termination to support installing the clamshell coupling directly over the insulation of a single conductor.

7. CONCLUSIONS

This report generally demonstrates that the inductive clamshell coupler can be used for online energized cable monitoring with virtually identical results as mechanical T-couplings to cable conductors under test. Test instruments are the same ones used for off-line monitoring, but the coupler protects the instruments from energized line high voltages that would normally damage the instruments. Online cable monitoring enables real-time continuous cable condition assessment without waiting for an outage or removing a system from service for test.

Specific conclusions are:

- The clamshell coupling permits the acquisition of FDR and SSTDR reflectometry data on live lines. Tests demonstrated suitable isolation up to the 6.7 kVp-p target and potentially higher.

- The clarity of indications using the clamshell coupler is similar to indications using direct coupling between the conductor under test and the measurement instrument.

- Practical operational advantages of the clamshell coupler include:
  - Not contacting the conductor
  - Able to install without disconnecting cable.

- Disadvantages of the coupler include:
  - Large coupling around the conductor
  - Need shield to be peeled back
  - Need access to single-phase conductor.

REFERENCES

A.H. Systems. 2023. "Injection Current Probe ICP-622." A.H. Systems, inc. Accessed on September 13, 2024. https://www.ahsystems.com/catalog/ICP-622.php.

Ahmed, N. H., and N. N. Srinivas. 1998. "On-line partial discharge detection in cables." *IEEE Transactions on Dielectrics and Electrical Insulation* 5 (2):181-188. https://doi.org/10.1109/94.671927.

Fluke. 2022. "FLUKE Digital Clamp Meter: Clamp-Jaw Jaw, CAT III 600V/CAT IV 300V, TRMS." W.W. Grainger, Inc. Accessed 03/15/24. https://www.grainger.com/product/FLUKE-Digital-Clamp-Meter-Clamp-20E891?opr=PLADS&analytics=FM%3APLA&a2c_sku_original=20E890.

Furse C., Y.C. Chung, C. Lo, and P. Pendayla. 2006. "A Critical Comparason Reflectometry Methods for Location of Wireing Faults." *Smart Structures and Systems* 2:25-46. https://doi.org/10.12989/sss.2006.2.1.025.

Glass, S. W., A. M. Jones, L. S. Fifield, and T. S. Hartman. 2016. *Bulk and Distributed Electrical Cable Non-Destructive Examination Methods for Nuclear Power Plant Cable Aging Management Programs.* Pacific Northwest National Laboratory PNNL-25634. Richland, WA. https://www.pnnl.gov/main/publications/external/technical_reports/PNNL-25634.pdf.

Glass, S. W., A. M. Jones, L. S. Fifield, T. S. Hartman, and N. Bowler. 2017. *Physics-Based Modeling of Cable Insulation Conditions for Frequency Domain Reflectometry (FDR).* Pacific Northwest National Laboratory PNNL-26493. Richland, Washington. https://www.pnnl.gov/main/publications/external/technical_reports/PNNL-26493.pdf.

Glass, S.W., L S. Fifield, and M Prowant. 2021. *PNNL ARENA Cable Motor Test Bed Update.* Pacific Northwest National Laboratory PNNL 31415. Richland, Washington. https://www.pnnl.gov/main/publications/external/technical_reports/PNNL-31415.pdf

Glass, S.W., L.S. Fifield, and N. Bowler. 2020. *Cable Nondestructive Examination Online Monitoring for Nuclear Power Plants.* Pacific Northwest National Laboratory PNNL 155612. Richland, Washington. https://lwrs.inl.gov/content/uploads/11/2024/03/Cable_NDE_Online_Monitoring.pdf.

Glass, S.W., A. Sriraman, M. Prowant, M.P Spencer, L.S. Fifield, and S. Kingston. 2022. *Nondestructive Evaluation (NDE) of Cable Anomalies using Frequency Domain Reflectometry (FDR) and Spread Spectrum Time Domain Reflectometry (SSTDR).* Pacific Northwest National Laboratory PNNL-33334. Richland, Washington. https://www.pnnl.gov/main/publications/external/technical_reports/PNNL-33334.pdf.

Glass, S.W., J R Tedeschi, M.P.; Spencer, J. Son, M. Elen, and L.S. Fifield. 2023. *Laboratory Instrument Software Controlled Spread Spectrum Time Domain Reflectometry for Electrical Cable Testing.* Pacific Northwest National Laboratory PNNL-34511. Richland, Washington.

Han, J., Y. Zhou, C. Yang, W. Zheng, X. Lu, Y. Wang, J. Han, and L. Geng. 2023. "Review of Research on Running Condition Monitoring of High Voltage Cables." *2023 IEEE 3rd International Conference on Power, Electronics and Computer Applications (ICPECA)*, 29-31 Jan. 2023. https://doi.org/10.1109/ICPECA56706.2023.10075700.

NRC. 2010. *Essential Elements of an Electric Cable Condition Monitoring Program (NUREG/CR7000, BNL-NUREG-90318-2009).* Nuclear Regulatory Commission. Washington, D.C.

Yao, Lijun, Weiyu Ma, and Canyi Yu. 2014. "Correlation between transfer impedance and insertion loss of current probes." *Electromagnetic Compatibility Magazine, IEEE* 3:51-55. https://doi.org/10.1109/MEMC.2014.6849544.